Water Assisted Reaction Mechanism of OH- with CCl4 in Aqueous Solution – Hybrid Quantum Mechanical and Molecular Mechanics Investigation

ARTICLE *in* CHEMICAL PHYSICS LETTERS · FEBRUARY 2013

Impact Factor: 1.9 · DOI: 10.1016/j.cplett.2012.12.058

4 AUTHORS, INCLUDING:

Dunyou Wang
Shandong Normal University
55 PUBLICATIONS **1,739** CITATIONS
SEE PROFILE

Marat Valiev
Pacific Northwest National Laboratory
85 PUBLICATIONS **2,132** CITATIONS
SEE PROFILE

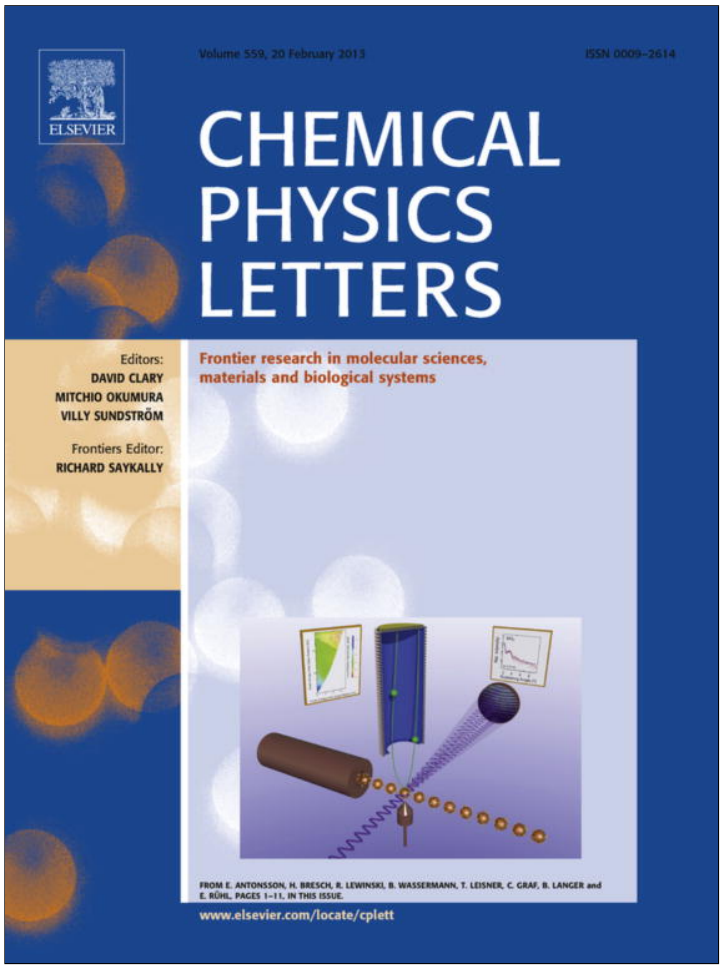

Chemical Physics Letters 559 (2013) 30–34

Contents lists available at SciVerse ScienceDirect

Chemical Physics Letters

journal homepage: www.elsevier.com/locate/cplett

Water assisted reaction mechanism of OH^- with CCl_4 in aqueous solution – Hybrid quantum mechanical and molecular mechanics investigation

Jie Chen [a], Hongyun Yin [a], Dunyou Wang [a,*], Marat Valiev [b,*]

[a] College of Physics and Electronics, Shandong Normal University, Jinan 250014, China
[b] Environmental Molecular Sciences Laboratory, Pacific Northwest National Laboratory, MS-IN K8-91, P.O. Box 999, Richland, WA 99352, USA

ARTICLE INFO

Article history:
Received 1 November 2012
In final form 28 December 2012
Available online 8 January 2013

ABSTRACT

The $OH^-(H_2O) + CCl_4$ reaction in aqueous solution was investigated using the combined quantum mechanical and molecular mechanics approach. The reaction mechanism of $OH^-(H_2O) + CCl_4$ consists of two concerted steps – formation of OH^- in the favorable attack conformation via the proton transfer process, and the nucleophilic substitution process in which the newly formed OH^- attacks the CCl_4. The free energy activation barrier is 38.2 kcal/mol at CCSD(T)/MM level of theory for this reaction, which is about 10.3 kcal/mol higher than that of the direct nucleophilic substitution mechanism of the $OH^- + CCl_4$ reaction in aqueous solution.

1. Introduction

The topic of solvent effects in solution has been a subject of great interest. Solvent effects can influence the reactant structures, alter the relative energies of reactant, transition, and product states, and greatly impact the reaction rate and mechanism. For example, the reaction rate constant of $Cl^- + CH_3Br$ in gas-phase is 15 orders of magnitude larger than that in water [1]. It is important to understand the solvent effects on reactions in solution, from the long-range interaction of the bulk solvent to the short-range interaction of the solvent molecule participation of the reaction, as well as nucleophile, leaving group and substituent effects on the reactivity.

Chlorinated organic compounds are a significant and expanding source of environmental contamination on the planet. They have been used as synthetic solvents extractants, cleaning agents, pesticides, and degreasers in a range of industrial applications for a very long time [2]. Concerns are growing over their increasing presence, persistence and toxicity in the environment. For example, on the US EPA designated priority pollutant list [3], polychlorinated alkanes now account for a significant fraction of organic chemicals. Therefore, it is important to study the reaction mechanism of those polychlorinated hydrocarbon (PCHC) reactions in the aqueous solution.

There have already been some theoretical [4–6] and experimental [7–9] studies about the chlorinated hydrocarbons (CHCs), they were mainly focus on $CH_{(4-n)}Cl_n + OH^-$ ($n = 1–4$) in gas phase, and some studies on the micro-solvated systems [10–15]. Recently we have studied the influences of solvent environment for the bimolecular nucleophilic substitution (S_N2) reaction of $CH_{(4-n)}Cl_n + OH^-$ ($n = 1–4$) [16–19] in water. These studies show that the solvent environment has a large impact on the reaction rate and mechanism. For example, the study of $CCl_4 + OH^-$ [16] using combined quantum mechanical/molecular mechanics (QM/MM) shows that the aqueous environment has a great impact on the reaction by raising the reaction barrier by 10.5 kcal/mol. In that study, the aqueous solution was treated with the molecular mechanics method and was regarded having the long-range interaction effects onto the reactants; while $CCl_4 + OH^-$ reactant was treated using the accurate quantum mechanics method. However, there have been no studies in aqueous solution addressing the implications of short-range interaction of solvent molecule with solute in reaction processes. In such case, the solvent molecules may take direct part in the bond breaking and formation process. As a result, they have to be treated as part of the reactant using the QM method.

In this work, we study the reaction mechanics of one solvent water taking part in the reaction process, $OH^-(H_2O) + CCl_4$, in aqueous solution. The combined quantum mechanical/molecular mechanics (QM/MM) approach [20,21] is employed to simulate the reaction mechanism in aqueous solution, where the one H_2O molecule is regarded as an integral part of the reaction mechanism. The additional H_2O, as a part of the reactant now, is also treated quantum–mechanically and thus has a freedom to undergo bond breaking and formation during the reaction process in water solution. In order to reduce the computational expense associated with free energy calculations on the high accuracy coupled cluster (CC) [22] level, we are using a multi-layered approach, which combines the effective electrostatic potential (ESP) [23] charge representation, density functional theory (DFT) [24] and coupled cluster (CC)

* Corresponding authors.
E-mail addresses: dywang@sdnu.edu.cn (D. Wang), marat.valiev@pnl.gov (M. Valiev).

0009-2614/$ - see front matter © 2013 Elsevier B.V. All rights reserved.
http://dx.doi.org/10.1016/j.cplett.2012.12.058

representations to achieve an accurate reaction pathway on the CC level.

Our objectives of this Letter are twofolds. First, we investigate the reaction mechanism of this one additional H_2O molecule assisted nucleophilic substitution reaction $OH^-(H_2O) + CCl_4$, in order to see how it differs from the $OH^- + CCl_4$ reaction mechanism in water. Our treatment is the first such study in an aqueous solution. The second objective is to compute the potential of mean force (PMF) of the new reaction mechanism and to see how one extra solution molecule taking part in the reaction will affect the PMF reaction pathway as well as reaction energetics.

2. Computational methodology and system setup

All the calculations of the reaction $OH^-(H_2O) + CCl_4$ in water were performed using the QM/MM capabilities of NWChem computational chemistry package [25]. The calculation methodology has already discussed in prior publications Refs. [16–19].

Our QM region consisted of CCl_4, OH^- and the additional H_2O molecule. Its initial geometry was adopted from the previous gas-phase studies [26]. The QM region was embedded into a 37.4 Å cubic box consisting of 1750 water molecules, which were treated as the MM region. QM representation was based on either on DFT or CCSD(T) level of theory, leading correspondingly to DFT/MM or CC/MM representations. DFT calculations utilized the B3LYP [27,28] exchange correlation functional, and the aug-cc-pvDZ basis is used for both the DFT and CCSD(T) calculations. Standard Amber force field [29] van der Waals parameters were used for the quantum region. The classical MM representation for water solution was based on SPC/E model [30], and the cutoff radius for classical interactions is 15 Å.

First, we optimized the initial geometry of the reactant complex in water, and then carried out the molecular dynamics simulation to equilibrate the solvent for 40 picoseconds at 298 K. Then, re-optimization was performed again on the full system, and the obtained stable structure was used as the starting point for all subsequent simulations.

In the next step, we determined the transition state of the reaction water solution. First, using the fully optimized reactant complex obtained in the step above as the starting point, an initial guess for the reaction pathway was generated by simulating the bond breaking of C–Cl and the bond formation of the C atom to the O atom in H_2O using constrained optimization, while all the other degrees of freedom in the QM region are freely evolving. The initial pathway from the reactant to product was refined using the nudged elastic band (NEB) [31] method in our QM/MM approach. Second, the top geometry with the highest energy on the NEB pathway was used for the saddle point search calculation. The located transition state structure in water solution was verified through numerical frequency calculation that showed one imaginary frequency. Then the reactant and product complexes were found by optimizing the corresponding displacements of the transition-state along the negative frequency mode. Third, using the obtained final reactant and product complexes, the NEB pathway was constructed again with 10 geometries along the reaction profile. Molecular dynamics simulations were performed on each NEB bead along the reaction pathway to equilibrate the solvent for 40 picoseconds. This step was repeated until the NEB reaction pathway in water solution converged.

Similar to our previous studies [16–19], we calculated free energy difference along the NEB pathway using multi-layered approach combining ESP, DFT, CC, representations

$$\Delta W^{CC}_{A,B} = (\Delta W^{CC\to DFT}_{A,A} - \Delta W^{CC\to DFT}_{B,B}) + (\Delta W^{DFT\to ESP}_{A,A} - \Delta W^{DFT\to ESP}_{B,B}) + \Delta W^{ESP}_{A,B} \quad (1)$$

Here the first and second term in the parentheses represent free energy difference for changing the description from the CC to DFT representation and from DFT to classical ESP representations at the fixed solute configuration (A or B), respectively. And the last term represents the free energy difference for changing solute configuration from A to B in the classical ESP/MM representation.

As mentioned above, 10 points were chosen along the free energy profile. Between each two points on the reaction pathway, the free energy difference between two adjacent NEB points for the ESP/MM representation was sampled for 50 picoseconds to reach convergence.

3. Results and discussions

3.1. Reaction mechanism

The optimized reactant complex in aqueous solution is shown in Figure 1. The characteristic feature of this reactant complex is that the presumed nucleophile, OH^-, is not in the optimal position with respect to CCl_4 substrate. That position is occupied by the water molecule with the R_{OC} distance of 3.78 Å, positioned inline with respect to Cl leaving group (OCCl angle of 176 degrees). There is a strong hydrogen bond interaction between this water and hydroxyl with the R_{OO} distance of 2.5 Å. We also observe slight elongation of OH bond in the water molecule, alluding to the possibility of the proton transfer.

The transition state (also shown in Figure 1) is the No. 5 bead on the NEB reaction pathway. Numerical QM/MM frequency calculations confirm the presence of single imaginary frequency of

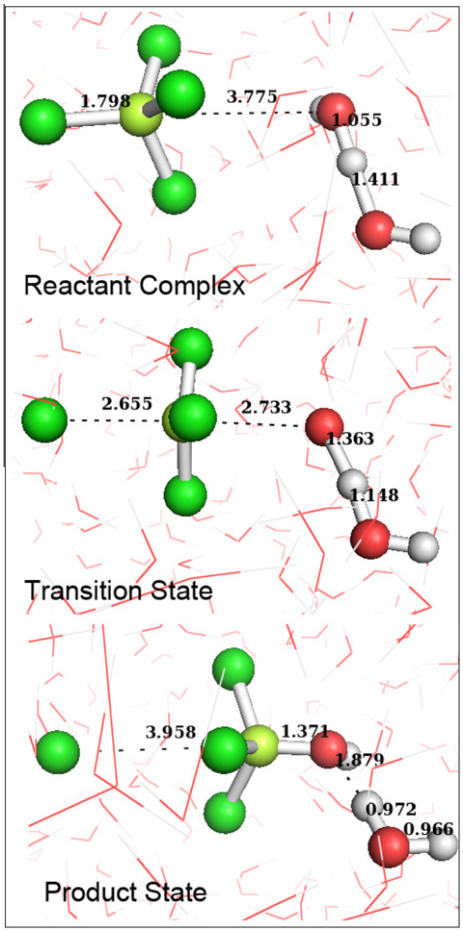

Figure 1. Reactant complex, transition state, and product complex of the $OH^-(H_2O) + CCl_4$ in water. All the bond lengths are in Angstroms.

332i cm^{-1}. Its structure is characteristic of two distinct events taking place. First, there is the proton transfer from water to hydroxyl, with net effect of creation of OH^- nucleophile in the optimal reaction configuration. The R_{OH-H} distance is 1.15 Å compared to 1.41 Å in the reactant state. The electron first attached to original OH^- in the reactant has been transferred to the new nucleophile. At the transition state, the electron further moves to circle around the whole transition state complex, rather than only locally attached to the new nucleophile. Second, we observe the Cl is leaving the center C atom with R_{CCl} distance of 2.66 Å (compared to 1.79 Å in the reactant state), caused by the movement CCl_3 group toward the nucleophile side, with inversion to nearly planar configuration. The overall distance between entering nucleophile and leaving group shows just a small contraction R_{OCl} of 5.38 Å (vs 5.57 Å in the reactant state)

In the product state (see Figure 1), the electron has been transferred to the Cl atom and the Cl^- leaving group is totally detached from the substrate (R_{ClC} = 3.96 Å) which now forms bond with the nucleophile on the opposite side (R_{CO} = 1.37 Å).

The evolution of specific bond distances is further analyzed in Figure 2A gives the bond breaking of C–Cl and bond formation of C–O which represents the nucleophilic substitution process. Figure 2B shows the forming of new nucleophile and the new H_2O which displays the proton transfer process. Comparing these two Figures, we can see that the proton transfer process develops a little faster than the nucleophilic substitution process before the transition state; nonetheless, both are ended at the bead number 10, the product state. Hence, for the whole reaction process, the two reaction mechanisms intertwine with each other and control the whole reaction mechanism—a proton transfer mechanism combined with the nucleophilic substitution mechanism. Here the additional H_2O molecule takes part in the bond breaking and formation process by transferring one proton to the original OH^- and producing the new OH^- to attack the C atom.

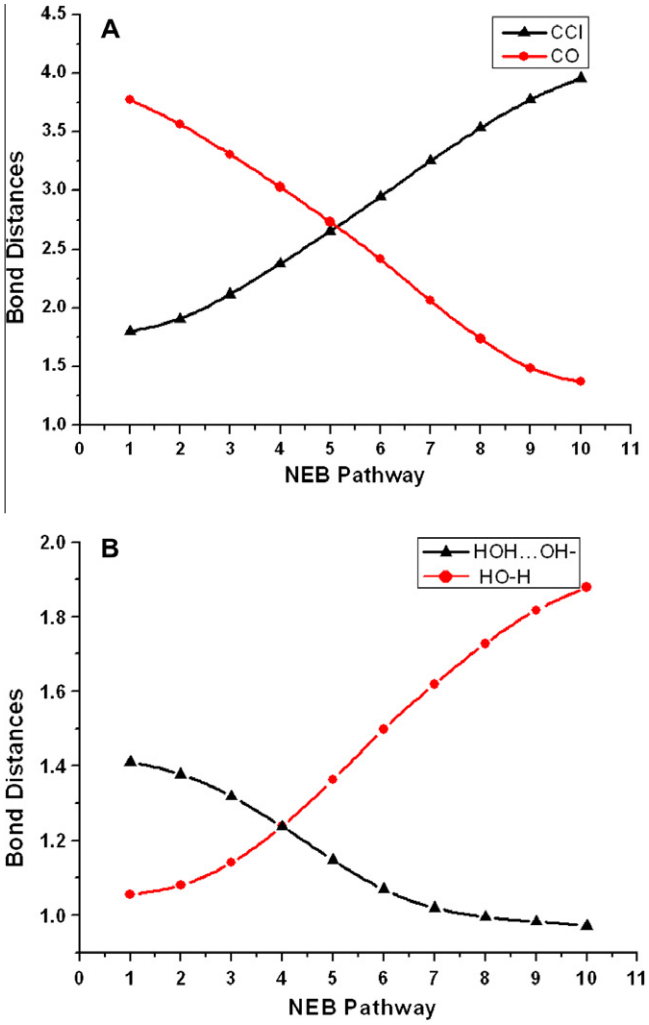

Figure 2. (A) shows the the nucleophilic substitution process represented by the evolution of C–O (here the O comes from H_2O) and Cl–C bond distances (Å) along the NEB reaction pathway. (B) Shows the proton transfer process represented by the evolution of HO–H in the original H_2O and the bond distance of HOH…OH^-.

Note the description of the dynamics of the bond breaking and formation process was based on the *ab initio* calculation for the evolution of the potential energy surface. However, since we allowed one extra H_2O to take part in the reaction process, the quantum effects of the nuclear motion may become very import to describe the reaction mechanism. Currently we do not have the ability to couple the nuclear motion quantum mechanically with the electron motion, thus we provide the reaction mechanism in a classical fashion without the nuclear quantum effects, such as the tunneling effect.

Comparing to the pure nucleophilic substitution reaction mechanism of the $OH^- + CCl_4$ reaction in water [16], the above reaction pictures illustrate that, with one extra H_2O molecule taking part in the reaction, the nucleophile OH^- does not attack the center C atom directly as in the $OH^- + CCl_4$ reaction. Since the extra water molecule in the reactant complex blocks the direct approach of the original nucleophile to the center C atom, thus the extra H_2O in the reactant inserts a steric effect to the original OH^- here. This steric effect has also been observed in the S_N2 micro-solvated reaction in gas-phase too [32]. Because the steric effect here hinders the nucleophilic substitution process, this title reaction needs one extra proton transfer process to 'assist' the nucleophilic substitution reaction.

In the current study, we only take one of the water molecules from the first hydration shell to be included in the reactants, which is treated quantum mechanically. Thus it has the ability to participate in the bond breaking and formation process. If more than one first hydration shell water molecules were treated quantum mechanically, the proton transfer process still need to occur to create a new OH^- to attach the center C atom, since the optimal attacking position is occupied by a water molecule. However, due to more than one H_2O molecules treated quantum mechanically, the proton transfer process might proceed via multiple water molecules. Nonetheless, here the proton transfer assisted reaction mechanism via a single water molecule should be one of the water assisted reaction mechanisms for this reaction in aqueous solution. Which one is the favorite reaction mechanism among the proton transfer assisted reaction mechanisms, via a single water molecule or multiple water molecules. This needs to be further investigated in the future.

3.2. Potential of mean force profiles

In Figure 3, we present the PMF along the NEB reaction pathway of the reaction $OH^-(H_2O) + CCl_4$ in water solution under the CCSD(T)/MM and DFT/MM representation, as well as the solvent contribution to the reaction which is the third term of Eq. (3). Here the number 1 bead on the PMF reaction pathway is used as the reference energy point, so only relative free energies along the pathway are calculated. Figure 3 also shows that the reaction barrier height for this reaction is 38.2 kcal/mol and the free energy of reaction is −38.4 kcal/mol under the CCSD(T)/MM representation in water solution. The reaction barrier for this title reaction in water solution is 10.3 kcal/mol higher than the one of the reaction $OH^- + CCl_4$ in water [16] at 27.9 kcal/mol. This can be explained from two

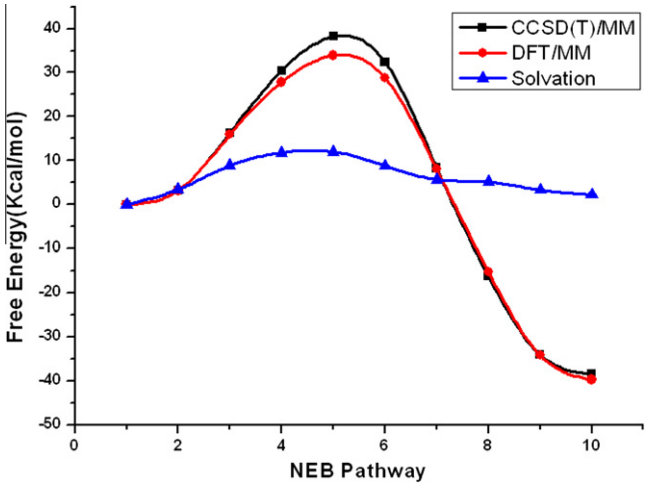

Figure 3. Comparison of the potential mean force along NEB reaction pathway. They are calculated at DFT/MM and CCSD(T)/MM levels of theory and solvation contribution using the reactant state (bead 1) as a reference point.

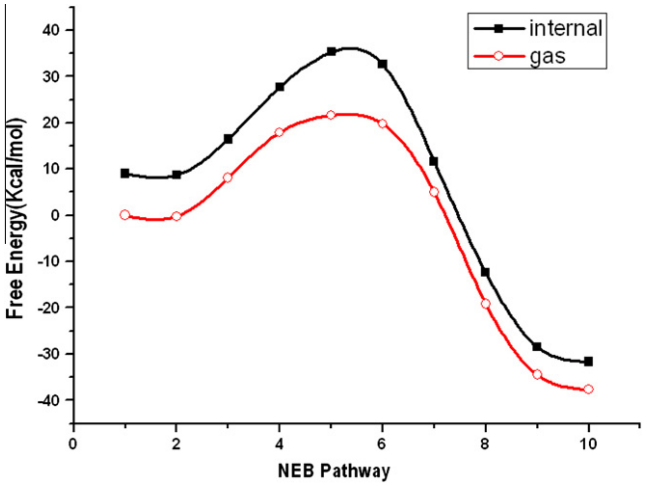

Figure 4. Comparison between gas-phase and internal QM/MM energies along the NEB pathway under the CCSD(T)/MM representation using the gas-phase energy of the reactant state as a reference point.

aspects: First, as the extra H_2O takes part in the reaction, it prohibits the original nucleophile OH^- to access the center C atom and exert a steric effect on the reaction, thus takes an extra proton transfer process to let the nucleophilic substitution reaction occur. Second, the extra H_2O molecule with OH^- happens to form an additional intramolecular hydrogen bonding. This intramolecular hydrogen bond weakens the inherent nucleophilicity, thus it increases the S_N2 reaction barrier directly. This feature has been found in Chen and Brauman's study of the intrinsic nucleophilicity of solvated nucleophiles [33].

The PMF free energy profile under the DFT/MM representation for this title reaction is also plotted against the one under the CCSD(T)/MM representation and the free energy contribution from the solvation effect in Figure 3. Our results show that the free energy activation barrier under the DFT/MM representation is 33.9 kcal/mol which is about 4 kcal/mol lower than the value under the CCSD(T)/MM representation. The free energy of reaction is −39.7 kcal/mol, which is 1.3 kcal/mol lower than that of the CCSD(T)/MM. The free energy lines under these two representations are very close to each other except at the transition state region and the product region.

By taking the current multilayer approach, the errors of the PMF calculation come from two sources: the first is from the statistical sampling of the water solution contribution to the PMF (the last term in Eq. (1). The variational computational uncertainty on the sampling is about ±0.4%, so the maximum estimated error bar is about ±0.05 kcal/mol on this part. The second is from the short vertical correction for the DFT as well as the CCSD(t) energies when the representations changed from DFT to ESP and from CC to DFT. However, we cannot estimate the vertical error at this point on the current calculation.

In order to study the polarization effects caused by the aqueous solution, we compare the gas phase and internal QM/MM energy under CCSD(T)/MM presentation in Figure 4 using the reactant state energy of the gas phase as the reference point. Note that the gas-phase reaction pathway is obtained by using the same 10 structures on the NEB reaction pathway in solution but excludes the interaction between the solute and solvent. This Figure shows the polarization effect does not change the overall shape of the curve of the NEB. However, compared with the gas phase, it contributes 8.9 kcal/mol to the reactant state, 13.6 kcal/mol to the transition state and 6.0 kcal/mol to the product state. These polarization effect contributions are smaller than those of the $CCl_4 + OH^-$ reaction at 11.5 kcal/mol and 15.5 kcal/mol for the reactant, transition state complex respectively, but larger than that of $CCl_4 + OH^-$ reaction at 3.08 kcal/mol for the product state compared to the gas-phase. This is because, at the reactant and transition state, with one additional H_2O presented in the nucleophile, the charge distributions are more dispersed than that of the $CCl_4 + OH^-$ reaction, resulting in a smaller polarization effect. However, at the product state, although all the negative charge is concentrated on the leaving group Cl^- which is the same for the two reactions, the presence of the additional H_2O molecules for the reaction of $CCl_4 + OH^-(H_2O)$ makes the polarization effect larger than that of the $CCl_4 + OH^-$ system.

4. Conclusion

A hybrid QM/MM method with multi-layered presentation DFT/MM, CCSD(T)/MM, and ESP/MM were employed to investigate the reaction mechanism of the $OH^-(H_2O) + CCl_4$ in aqueous solution. The reactant complex, transition state and produce state were determined and characterized and the reaction pathway for this reaction is also quantitatively obtained under the CCSD(T)/MM and DFT/MM representations. The detailed plots of reaction geometries of the NEB beads along the reaction pathway showed a concerted proton transfer and S_N2 nucleophilic substitution reaction mechanism. The activation barrier calculated under CCSD(T)/MM representation is 38.2 kcal/mol, which is 10.3 kcal/mol higher than that of $CCl_4 + OH^-$.

Acknowledgements

D. Wang thanks the National Natural Science Foundation of China (Grant #:11074150) and Tanshai Scholarship funding for supporting this work. The calculation was performed on the Magic Super Computer at Shanghai Supercomputer Center. Research at PNNL was also supported by the U. S. Department of Energy's (DOE) Office of Basic Energy Sciences, PNNL is operated by Battelle for DOE.

Reference

[1] J.H. Bowie, Acc. Chem. Res. 13 (1980) 76.
[2] S. Re, K. Morokuma, J. Phys. Chem. A 115 (2001) 7185.

[3] A.L. Roberts, P.M. Jeffers, N.L. Wolfe, P.M. Gschwend, Crit. Rev. Environ. Sci. Technol. 23 (1993) 1.
[4] K. Ohta, K. Morokuma, J. Am. Chem. Soc. 89 (1987) 5845.
[5] J.D. Evanseck, J.F. Blake, W.L. Jorgensen, J. Am. Chem. Soc. 109 (1987) 2349.
[6] (a) J.R. Pliego, W.R.D. Almeida, J. Phys. Chem. 100 (1996) 12410;
(b) J.R. Pliego, W.R.D. Almeida, Chem. Phys. Letts. 249 (1996) 136.
[7] (a) J. Hine, J. Am. Chem. Soc. 72 (1954) 2438;
(b) J. Hine, A.M. Dowell, J. Am. Chem. Soc. 76 (1954) 2688.
[8] M. Henchman, P.M. Hierl, J.F. Paulson, J. Am. Chem. Soc. 107 (1985) 2812.
[9] P.M. Hierl, J.F. Paulson, M. Henchman, J. Phys. Chem. 99 (1995) 15655.
[10] I. Adamovic, M.S. Gordon, J. Phys. Chem. A 109 (2005) 1629.
[11] H. Tachikawa, M. Igarashi, T. Ishibashi, Chem. Phys. Lett. 363 (2002) 335.
[12] H. Tachikawa, J. Phys. Chem. A 104 (2000) 497.
[13] S.J. Mo, T. Vreven, B. Mennucci, K. Morokuma, J. Tomasi, Theor. Chem. Acc. 111 (2004) 154.
[14] Y. Okuno, J. Chem. Phys. 105 (1996) 5817.
[15] R. Otto et al., Faraday Discuss. 157 (2012) 41.
[16] T.T. Wang, H.Y. Yin, D.Y. Wang, M. Valiev, J. Phys. Chem. A 116 (2012) 2371.
[17] M. Valiev, B.C. Garrett, M.-K. Tsai, K. Kowalski, S.M. Kathmann, G.K. Schenter, M. Dupuis, J. Chem. Phys. 127 (2007) 051102.
[18] D. Wang, M. Valiev, B.C. Garrett, J. Phys. Chem. A 115 (2011) 1380.
[19] H.Y. Yin, D.Y. Wang, M. Valiev, J. Phys. Chem. A 115 (2011) 12047.
[20] M. Valiev, K. Kowalski, J. Chem. Phys. 125 (2006) 211101.
[21] M. Valiev et al., J. Chem. Phys. 127 (2007) 051102.
[22] R.J. Bartlett, M. Musial, Rev. Mod. Phys. 79 (2007) 271.
[23] Y.K. Zhang, H.Y. Liu, W.T. Yang, J. Chem. Phys. 112 (2000) 3483.
[24] P. Hohenberg, W. Kohn, Phys. Rev. 140 (1965) A1133.
[25] M. Valiev et al., Comput. Phys. Commun. 181 (2010) 1477.
[26] S. Re, Theor. Chem. Acc. 112 (2004) 59.
[27] A.D. Becke, J. Chem. Phys. 98 (1993) 5648.
[28] C. Lee, W. Yang, R.G. Parr, Phys. Rev. B 37 (1988) 785.
[29] T. Fox, P.A. Kollman, J. Phys. Chem. B 102 (1998) 8070.
[30] H.J.C. Berendsen, J.R. Grigera, T.P. Straatsma, J. Phys. Chem. 91 (1987) 6269.
[31] G. Henkelman, B.P. Uberuaga, H. Jonsson, J. Chem. Phys. 113 (2000) 9901.
[32] G. Caldwell, T.F. Magenera, P. Kebarke, J. Am. Chem. Soc. 106 (1984) 959.
[33] X. Chen, J.I. Brauman, J. Am. Chem. Soc. 130 (2008) 15038.